

Half-Quantum Vortex Pair in Polar-distorted B Phase of Superfluid ^3He in Aerogels

Masaki Tange and Ryusuke Ikeda

Department of Physics, Graduate School of Science, Kyoto University, Kyoto 606-8502, Japan

(Dated: March 1, 2022)

Motivated by the recent observation and argument on a large half-quantum vortex (HQV) pair connected by a Kibble wall in superfluid ^3He in nematic aerogels, we numerically study to what extent a huge HQV pair can intrinsically occur with no pinning effect due to the aerogel structure in the polar-distorted B (PdB) phase of superfluid ^3He . By fully examining the impurity-scattering induced pairing vertex, the emergence of Anderson's Theorem in the p -wave superfluid is verified in the two opposite limits, the isotropic and strongly anisotropic limits. Solving numerically the resulting Ginzburg-Landau (GL) free energy in the weak-coupling approximation and by taking account of the Fermi-liquid (FL) corrected gradient terms, the anisotropy dependence of the vortex structure minimizing the free energy is examined. It is found that, close to the transition between the polar and PdB phases, an interplay of the strong anisotropy and the FL correction makes emergence of a large HQV pair in the PdB phase possible, and that, nevertheless, such a large pair easily shrinks deep in the PdB phase, indicating that a pinning effect due to the aerogel structure is necessary in order to keep a large pair size there. The obtained result indicates the validity of the London limit for describing the vortex structure, and a consistency with the picture based on the NMR measurement is discussed.

PACS numbers:

I. INTRODUCTION

The recent observation of half-quantum vortices (HQVs) [1] in the polar superfluid phase, proposed to appear in superfluid ^3He in anisotropic aerogels through a model calculation [2] assuming a weak anisotropy and experimentally discovered in nematic aerogels [3], has opened a new door for studying possible vortices in a fermionic superfluid phase. A nematic aerogel has its strands aligned to one direction and can be regarded, broadly speaking, as a collection of line-like obstacles. The HQV has originally been expected to be realized in the thin film configuration of the chiral superfluid A phase with its orbital angular momentum locked perpendicularly to the film plane [4, 5]. However, the chiral A phase is realized with the help of the strong-coupling correction which is effective at higher pressures, while it has been clarified [6] that the HQV tends to be destabilized by the strong coupling correction. Fortunately, the polar phase realized in the nematic aerogel has a wider temperature range of its stability at relatively lower pressures, and hence, a superfluid ^3He in the nematic aerogels becomes the best playground for studying this novel topological object.

Recently, experimental investigation on the vortices in the nematic aerogel has been extended to lower temperatures [7], and the HQVs have been found through the NMR measurements to survive in the A and B phases realized at lower temperatures in the nematic aerogels. Since such A and B phases in the nematic aerogel are distorted by the anisotropy of the scattering events due to the aerogel structure, the resulting A and B phases will be called hereafter as the polar-distorted A (PdA) and PdB phases following Ref.[7]. It has been suggested that the detected HQV-pairs do not change their positions upon both the cooling from and the warming to

the polar phase, and hence that, since in their rotated experiments the rotation axis is parallel to the direction to which the strands are aligned, realization of such surprising events is largely supported by a strong pinning effect due to the line-like aerogel structure [7]. There, however, just the method of analyzing the NMR data on the basis of a hypothetical description of the vortex structure in the London limit has been presented, and the validity of their London description has not been examined. We note that a similar anisotropic growth of the half-core structure of the double-core vortex occurring upon cooling in the context of the superfluid ^3He in *isotropic* aerogels cannot be described based on the London limit [8]. Therefore, it is natural to ask to what extent the huge HQV pairs realized in the PdA and PdB phases are intrinsically stable and whether the description in the London limit is justified or not.

In the present work, we start with reformulating the Ginzburg-Landau (GL) approach for describing the superfluid ^3He in anisotropic aerogels by extending the weakly anisotropic model [2] of the impurity-scattering potential to the strongly anisotropic case appropriate for the situations in the nematic aerogel [1, 3, 9]. Using the resulting GL free energy, stable vortex solutions are studied in both the polar and PdB phases in strongly anisotropic cases. Throughout this work, we focus on the weak-coupling approximation neglecting the strong-coupling correction to the bulk free energy terms because incorporating the strong-coupling correction in the strongly anisotropic case has not been formulated so far. For this reason, the PdA phase never appears in the present results, and we have only a direct continuous transition between the polar and PdB pairing states. Since our model covers, in the weak-coupling approximation, the well-known isotropic case which has essentially the same vortex solution as in the bulk liquid case,

we study how the nonaxisymmetric double-core vortex is changed and stabilized with increasing the anisotropy on the impurity-scattering process. The core structure of the double-core vortex is often called as a half-core pair, because, under an appropriate condition, the description of the half-core pair based on the London limit, i.e., a HQV pair connected by a planar wall [10] becomes appropriate. Throughout this work, the double-core vortex will be identified with a HQV pair *only when the planar wall is well defined and clearly visible*. It is found that, as the anisotropy is increased, the description in the London limit of the order parameter profiles of one HQV-pair becomes better. Further, as the anisotropy is increased, the separation between the two HQVs forming one pair is increased and, in particular, becomes macroscopic close to the transition temperature T_{PB} between the polar and PdB phases. However, this size rapidly shrinks upon cooling from T_{PB} , accompanying an increase of the tension of the Kibble wall of the polar-distorted planar state [11] upon cooling. It implies that, deep in the PdB phase, a HQV pair with a macroscopic size is not naturally stabilized and hence, justifies the picture [7] of a HQV pair stabilized by the pinning due to the line-like aerogel structure.

The present paper is organized as follows. In sec.II, the vertex correction to the pairing process is explained in details together with the model of the impurity scattering used in this work. In sec.III, the resulting GL free energy affected by the impurity effects is explained. In sec.IV, it is explained how a HQV pair in the PdB phase is stabilized within the description in the London limit. Our numerical results and detailed discussions about them are presented in sec.V, and a summary and discussions are given in sec.VI. Details on the impurity-induced vertex correction and its effects on the $O(|\Delta|^4)$ gradient terms are explained in two Appendices.

II. MODEL OF IMPURITY SCATTERING

Our microscopic analysis for deriving the GL free energy is based on a BCS Hamiltonian with the nonmagnetic and random scattering potential term of the form

$$\mathcal{H}_{\text{imp}} = \int_{\mathbf{r}} \psi_{\sigma}^{\dagger}(\mathbf{r}) u(\mathbf{r}) \psi_{\sigma}(\mathbf{r}). \quad (1)$$

Here we focus on the case in which the scattering process is nonmagnetic, since the local surface of the aerogel is implicitly assumed to be entirely coated by ^4He so that the spin-flip scattering between the solid ^3He on the surface and the quasiparticles of the liquid ^3He is ineffective. Regarding the random averaging over $u(\mathbf{r})$, the Fourier transform $u(\mathbf{k})$ of $u(\mathbf{r})$ is assumed to have zero mean and the mean-squared average

$$\overline{|u_{\mathbf{k}}|^2} = \frac{1}{2\pi N(0)\tau} w(\mathbf{k}). \quad (2)$$

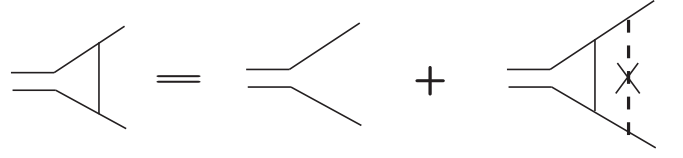


FIG. 1: Diagram expressing the Bethe-Salpeter equation the vertex function Λ (triangle) obeys. The straight solid lines mean normal Green's functions, and the impurity average of the squared random potential is expressed by a dashed line with a cross.

In the original work [2], a weak anisotropy has been incorporated in $w(\mathbf{k})$ in the form

$$w(\mathbf{k}) = 1 - \delta \hat{k}_z^2, \quad (3)$$

where $\hat{k}_z = k_z/k_F$. The positive constant δ in eq.(3) corresponds to $-\delta_u$ in Ref.[2] where a narrow polar phase has been proposed to appear in an aerogel sample stretched along the z -direction. For this reason, the z -axis will be called as the polar axis. Hereafter, as an extension of this impurity-scattering model to the case in a strongly anisotropic aerogel, the following model on $w(\mathbf{k})$ will be used:

$$w(\mathbf{k}) = \frac{1 + (\sqrt{\delta} - 1)\theta(\delta - 1)}{1 + \delta \hat{k}_z^2}. \quad (4)$$

In the weakly anisotropic limit where $\delta \ll 1$, this expression reduces to eq.(3), while, in the opposite strongly anisotropic limit where $\delta \rightarrow +\infty$, eq.(4) approaches the quantity

$$w_{\infty}(\mathbf{k}) = \pi k_F \delta(k_z). \quad (5)$$

The factor $\sqrt{\delta}$ in eq.(4) in $\delta \geq 1$ is necessary to obtain a physically reasonable limit of the quasiparticle relaxation rate in $\delta \rightarrow \infty$. Equation (5) implies that, in the limit of strong anisotropy, the scattering event is specular along the polar axis. This corresponds to the model proposed by Fomin [12] regarding the nematic aerogels as a collection of columnar defects.

To derive a GL free energy incorporating the scattering processes via the anisotropic aerogel structure with any strength of the anisotropy, we need a renormalized pairing vertex Λ_j replacing the bare pairing vertex $\hat{p}_j = p_j/k_F$, which depends not only on the relative momentum \mathbf{p} but also on the center-of-mass momentum \mathbf{k} and the fermion Matsubara frequency ε . The Bethe-Salpeter equation sketched in Fig.1

$$\begin{aligned} \Lambda_j(\hat{\mathbf{p}}; \mathbf{k}) &= \hat{p}_j + \frac{1}{2\pi N(0)\tau} \int_{\mathbf{p}'} \Lambda_j(\hat{\mathbf{p}}'; \mathbf{k}) \\ &\times \mathcal{G}_{\varepsilon}(\mathbf{p}' + \mathbf{k}/2) \mathcal{G}_{-\varepsilon}(-\mathbf{p}' + \mathbf{k}/2) w(\mathbf{p} - \mathbf{p}') \end{aligned} \quad (6)$$

for Λ_j can be solved in a closed form by assuming Λ_j to take the expression

$$\Lambda_j(\hat{\mathbf{p}}; \mathbf{k}) = \hat{p}_j(\delta_{ij}^{(z)} + \hat{z}_j(\hat{z}_i C(\mathbf{k}) + vk_i vk_z C_{1z})) - is_\varepsilon vk_j(\delta_{ij}^{(z)} B(\hat{p}_z) + \hat{z}_i \hat{z}_j (B(\hat{p}_z) + D(\hat{p}_z)))(\mathbf{k}),$$

where $\delta_{ij}^{(z)} = \delta_{ij} - \hat{z}_i \hat{z}_j$, $s_\varepsilon = \varepsilon/|\varepsilon|$, vp_j is the Fermi velocity, and

$$\begin{aligned} C(\mathbf{k}) &= C_0(\varepsilon) + C_{21}(\varepsilon)v^2 k^2 + C_{2z}(\varepsilon)v^2 k_z^2, \\ B(\hat{p}_z) &= B_0(\varepsilon) + \Delta B(\varepsilon)\hat{p}_z^2, \\ D(\hat{p}_z) &= D_0(\varepsilon) + \Delta D(\varepsilon)\hat{p}_z^2. \end{aligned} \quad (8)$$

The general form of Λ_j is involved and will be presented in Appendix. Here, just its limiting expressions will be explained. First, in the isotropic limit where $\delta \rightarrow 0$, $C_0 \rightarrow 1$, and other coefficients except B_0 vanish. Then, Λ_j reduces to

$$\Lambda_j^{(0)} = \delta_{ij} \left(\hat{p}_j - is_\varepsilon vk_j \frac{1}{12\tau|\varepsilon\tilde{\varepsilon}_0|} \right), \quad (9)$$

where $|\tilde{\varepsilon}_0| = |\varepsilon| + 1/(2\tau)$. As stressed elsewhere [8], the divergent behavior proportional to $|\varepsilon|^{-1}$ in the second term is a consequence of cancellation between the quasiparticle relaxation rate and the impurity-ladder vertex correction and is the origin of the impurity scattering-independent transition temperature in the s -wave superconductor. In this sense, this cancellation may be regarded as one analog of the Anderson's theorem [13, 14] in the s -wave superconductor.

In the opposite limit where $\delta \rightarrow +\infty$, i.e., the limit of strong anisotropy, the coefficients in Λ_j have the following limiting values:

$$\begin{aligned} B_0 &\simeq -\Delta B = -D_0 = \frac{\pi}{16|\varepsilon\tilde{\varepsilon}_\infty|\tau}, \\ \Delta D &\simeq -D_0 + \frac{\pi}{8\varepsilon^2\tau}, \\ C_0 &\simeq \frac{|\tilde{\varepsilon}_\infty|}{|\varepsilon|}, \\ C_{21} &\simeq -\frac{\pi}{32\varepsilon^2|\tilde{\varepsilon}_\infty|\tau}, \\ C_{1z} &\simeq -\frac{\pi}{16\tilde{\varepsilon}_\infty^2|\varepsilon|\tau} \left(1 + \frac{\pi}{8|\varepsilon|\tau} \right), \end{aligned} \quad (10)$$

and $C_{2z} = -C_{21} - C_{1z}$, where $|\tilde{\varepsilon}_\infty| = |\varepsilon| + \pi/(4\tau)$. Then, Λ_j approaches

$$\begin{aligned} \Lambda_j^{(\infty)} &= \delta_{ij}^{(z)} (\hat{p}_j - is_\varepsilon \frac{\pi}{16|\varepsilon\tilde{\varepsilon}_\infty|\tau} vk_j \hat{p}_\perp^2) + \hat{z}_i \hat{z}_j \frac{|\tilde{\varepsilon}_\infty|}{|\varepsilon|} \\ &\times \left[\hat{p}_j \left(1 - \frac{\pi}{32\tilde{\varepsilon}_\infty^2|\varepsilon|\tau} v^2 k_\perp^2 \right) - is_\varepsilon \hat{p}_z^2 \frac{\pi}{8|\varepsilon\tilde{\varepsilon}_\infty|\tau} vk_j \right] \\ &- \delta_{ij}^{(z)} \mathbf{k}_j \frac{\pi}{16\tilde{\varepsilon}_\infty^2|\varepsilon|\tau} \left(1 + \frac{\pi}{8|\varepsilon|\tau} \right) v^2 \hat{p}_z k_z \end{aligned} \quad (11)$$

where $\hat{p}_\perp^2 = 1 - \hat{p}_z^2$. We note that the second term of $|\tilde{\varepsilon}_\infty|$ corresponds to the imaginary part of the self energy of the normal Green's function. The k_\perp^2 term in eq.(11) suggests the presence of a diffusion pole $(2|\varepsilon| + v^2\tau k^2/\pi)^{-1}$. Consequences of $\Lambda_j^{(\infty)}$ are reflected in each term of the GL free energy which will be given in the next section and Appendices.

III. RESULTING GL FREE ENERGY

We will use an appropriate GL free energy to numerically study the vortex solutions stable in anisotropic aerogels. As has been assumed in Ref.[6], the terms arising from spatial variations of the superfluid transition temperature T_c and acting as a pinning potential of a vortex will be neglected in the free energy terms written by the order parameter field $A_{\mu i}$. Further, any term associated with the repulsive channel of the quasiparticle interaction will be neglected in this section. Then, the GL free energy $F_{\text{GL}} = F_2 + F_4$ in the presence of the impurity-scattering effect, as usual, consists of the quadratic term

$$\begin{aligned} F_2 &= -\frac{1}{2} \int_{\mathbf{q}} \int_{\mathbf{p}} T \sum_{\varepsilon} \Lambda_i(\varepsilon, \hat{p}, q) \mathcal{G}_{\varepsilon}(\mathbf{p} + \mathbf{q}/2) \mathcal{G}_{-\varepsilon}(-\mathbf{p} + \mathbf{q}/2) \\ &\times \hat{p}_j \text{tr}[\sigma_{\mu} \sigma_{\nu}] A_{\mu i}^*(\mathbf{q}) A_{\nu j}(\mathbf{q}) \end{aligned} \quad (12)$$

and the quartic term

$$\begin{aligned} F_4/\Omega &= \frac{1}{2} [A_{\mu i}^* A_{\mu j} A_{\nu k}^* A_{\nu l} - A_{\mu i}^* A_{\nu j} A_{\mu k}^* A_{\nu l} + A_{\mu i}^* A_{\nu j} A_{\nu k}^* A_{\mu l}] \\ &\times T \sum_{\varepsilon} \int_{\mathbf{p}_1} \int_{\mathbf{p}_2} \int_{\mathbf{p}_3} \int_{\mathbf{p}_4} \Lambda_i(\varepsilon, \mathbf{p}_1) \Lambda_j(\varepsilon, \mathbf{p}_2) \Lambda_k(\varepsilon, \mathbf{p}_3) \Lambda_l(\varepsilon, \mathbf{p}_4) \mathcal{G}_{\varepsilon}(\mathbf{p}_1) \mathcal{G}_{-\varepsilon}(-\mathbf{p}_1) \mathcal{G}_{\varepsilon}(\mathbf{p}_3) \mathcal{G}_{-\varepsilon}(-\mathbf{p}_3) \\ &\times \left(\delta_{p_1 p_2} \delta_{p_1 p_3} \delta_{p_1 p_4} + \delta_{p_1 p_4} \delta_{p_2 p_4} \mathcal{G}_{\varepsilon}(\mathbf{p}_1) \mathcal{G}_{\varepsilon}(\mathbf{p}_2) \overline{|u_{\mathbf{p}_1 - \mathbf{p}_2}|^2} + \delta_{p_1 p_2} \delta_{p_3 p_4} \mathcal{G}_{\varepsilon}(\mathbf{p}_1) \mathcal{G}_{\varepsilon}(\mathbf{p}_3) \overline{|u_{\mathbf{p}_1 - \mathbf{p}_3}|^2} \right), \end{aligned} \quad (13)$$

where Ω is the volume, and, for simplicity, the spatial variation of the order parameter was neglected in writing F_4 . Up to the lowest order in the spatial gradient, one can separate $F_2 + F_4$ into the bulk energy contribution $F_{\text{bulk}} = \int_{\mathbf{r}} f_{\text{bulk}}$, where

$$\begin{aligned} f_{\text{bulk}} = & (\alpha + (\alpha_z - \alpha)\delta_{iz})A_{\mu i}A_{\mu i}^* + \beta_1^{(0)}|A_{\mu i}A_{\mu i}|^2 + \beta_2^{(0)}(A_{\mu i}A_{\mu i}^*)^2 + \beta_3^{(0)}A_{\mu i}^*A_{\nu i}^*A_{\mu j}A_{\nu j} \\ & + \beta_4^{(0)}A_{\mu i}^*A_{\nu i}^*A_{\mu j}^*A_{\nu j} + \beta_5^{(0)}A_{\mu i}^*A_{\nu i}^*A_{\mu j}^*A_{\nu j} + \beta_z|A_{\mu z}A_{\mu z}|^2 \\ & + [\beta_1^{(1)}A_{\mu i}A_{\mu i}^*A_{\mu z}^*A_{\mu z} + \beta_2^{(1)}A_{\mu i}A_{\mu i}^*A_{\mu z}^*A_{\mu z} + \beta_3^{(1)}A_{\mu i}^*A_{\nu i}^*A_{\mu z}A_{\nu z} \\ & + \beta_4^{(1)}A_{\mu i}^*A_{\nu i}^*A_{\mu z}A_{\nu z} + \beta_5^{(1)}A_{\mu i}^*A_{\nu i}^*A_{\mu z}A_{\nu z} + \text{c.c.}], \end{aligned} \quad (14)$$

and the gradient terms. In the case of weak anisotropy where $\delta \ll 1$, the $\beta_n^{(1)}$ ($n = 1, \dots, 5$) terms appear in $O(\delta)$, while β_z term first appears in $O(\delta^2)$.

Among the gradient terms, the free energy density corresponding to the contributions from F_2 consist of the following seven terms:

$$\begin{aligned} f_{\text{grad}} = & 2K_1\partial_i A_{\mu i}\partial_j A_{\mu j}^* + K_2\partial_i A_{\mu j}\partial_i A_{\mu j}^* + K_3\partial_z A_{\mu i}\partial_z A_{\mu i}^* \\ & + K_4\partial_i A_{\mu z}\partial_i A_{\mu z}^* + K_5(\partial_i A_{\mu i}\partial_z A_{\mu z}^* + \text{c.c.}) \\ & + K_6\partial_z A_{\mu z}\partial_z A_{\mu z}^*. \end{aligned} \quad (15)$$

General expressions on the coefficients in the GL free energy are involved and will be presented in Appendix. Here, their limiting behaviors in the limits of weak anisotropy, $\delta \rightarrow 0$, and of strong anisotropy, $\delta \rightarrow \infty$ will be explained together with their implication. In $\delta \rightarrow 0$ limit, up to $O(\delta)$, β_z vanishes, and the remaining GL coefficients of f_{bulk} reduce to those given in Ref.[2]. In the isotropic ($\delta \rightarrow 0$) limit, the four coefficients of f_{grad} , K_j ($j = 3, \dots, 6$), vanish, while K_1 and K_2 coincide with those given in Ref.[8]. Among them, K_1 logarithmically diverges upon cooling, reflecting the cancellation between the relaxation rate and the pairing vertex mentioned in sec.II.

In contrast, in the $\delta \rightarrow \infty$ limit, the coefficients in f_{bulk} have the following limiting values :

$$\begin{aligned} \alpha & \simeq \frac{1}{3}N(0)\left[\ln\left(\frac{T}{T_{c0}}\right) + \psi\left(\frac{1}{2} + \frac{1}{8\tau T}\right) - \psi\left(\frac{1}{2}\right)\right], \\ \alpha_z & \simeq \frac{1}{3}N(0)\ln\left(\frac{T}{T_{c0}}\right), \end{aligned} \quad (16)$$

$$\begin{aligned} \beta_3^{(0)} & = -2\beta_1^{(0)} \simeq \frac{\pi T}{15}N(0)\sum_{\varepsilon>0}\frac{1}{|\tilde{\varepsilon}_{\infty}|^3}, \\ \beta_2^{(0)} & = \beta_4^{(0)} = -\beta_5^{(0)} \simeq \beta_3^{(0)} - \frac{\pi^2 T}{60\tau}N(0)\sum_{\varepsilon>0}\frac{1}{\tilde{\varepsilon}_{\infty}^4}, \\ \beta_3^{(1)} & = -2\beta_1^{(1)} \simeq -\beta_3^{(0)} + \frac{\pi T}{15}N(0)\sum_{\varepsilon>0}\frac{1}{\varepsilon^2|\tilde{\varepsilon}_{\infty}|}, \\ \beta_2^{(1)} & = \beta_4^{(1)} = -\beta_5^{(1)} \simeq \beta_3^{(1)} + \frac{\pi^2 T}{60\tau}N(0)\sum_{\varepsilon>0}\frac{1}{\tilde{\varepsilon}_{\infty}^4}\left(1 - \frac{\tilde{\varepsilon}_{\infty}^2}{2\varepsilon^2}\right), \\ \beta_{12345}^{(0)} & + 2\beta_{12345}^{(1)} + \beta_z \simeq \frac{\pi T}{10}N(0)\sum_{\varepsilon>0}\frac{1}{|\varepsilon|^3}, \end{aligned} \quad (17)$$

where $\beta_{12345} = \beta_1 + \beta_2 + \beta_3 + \beta_4 + \beta_5$. It can be verified that $\beta_n^{(1)}$ and β_z vanish in the true clean limit where $\tau^{-1} = 0$.

The fact that α_z approaches its result in the impurity-free bulk liquid is a consequence of the specular scattering along the polar axis (see eq.(5)) and implies that the superfluid transition temperature T_c between the normal phase and the polar pairing state is not affected by the impurity scattering in the limit of strong anisotropy. Thus, this α_z -expression can be regarded as another analog of the Anderson's theorem [13] in the s -wave superconductor [12, 15, 16]. Consistently with the behavior of α_z , the last line of eq.(17) which is the coefficient of the quartic bulk term associated with the description of the polar phase also becomes independent of τ . Therefore, the squared amplitude of the order parameter $|\Delta_{\text{polar}}|^2 = A_{\mu z}^*A_{\mu z}$ which becomes $-\alpha_z/(\beta_{12345}^{(0)} + 2\beta_{12345}^{(1)} + \beta_z)$ within the present GL treatment is also independent of τ [15]. Such an impurity-free nature at the polar to normal transition does not hold at the transition temperature to another pairing state at lower temperatures [12, 16].

As stressed elsewhere [16], the above-mentioned impurity-free thermodynamic behavior of the polar pairing state at finiet temperatures is approximatedly seen if $\delta \geq 5$. So, even in aerogels to be modelled by a finite δ , the model in the limit of strong anisotropy can be conveniently used for theoretical descriptions.

Due to the nonvanishing δ , as seen in eq.(15), the quadratic gradient energy f_{grad} consists of the six invari-

ants, and the corresponding six coefficients remain non-vanishing even in the limit of strong anisotropy ($\delta \rightarrow \infty$). In low T limit, all coefficients remain nonvanishing, and their leading terms in low T limit become

$$\begin{aligned} K_1 &\simeq \frac{\pi^2 T v^2}{120} N(0) \sum_{\varepsilon > 0} \frac{1}{|\varepsilon| |\tau| |\tilde{\varepsilon}_\infty|^3}, \\ K_4 &\simeq \frac{\pi^2 T v^2}{48} N(0) \sum_{\varepsilon > 0} \frac{1}{|\varepsilon|^2 |\tau| |\tilde{\varepsilon}_\infty|^2}, \\ K_5 &\simeq \frac{\pi^2 T v^2}{480} N(0) \sum_{\varepsilon > 0} \frac{1}{|\varepsilon|^2 |\tau| |\tilde{\varepsilon}_\infty|^2} \left(1 + \frac{5}{4} \frac{\pi}{|\tilde{\varepsilon}_\infty| |\tau|} \right). \end{aligned} \quad (18)$$

Further, the coefficient of $\partial_z A_{\mu z}^* \partial_z A_{\mu z}$ which arises from the sum of the K_4 , K_5 , and K_6 terms approaches

$$\frac{\pi^2 T v^2}{80} N(0) \sum_{\varepsilon > 0} \frac{1}{\varepsilon^2 \tilde{\varepsilon}_\infty^2 \tau}. \quad (19)$$

The divergent behaviors $\sim \varepsilon^{-2}$ in low T limit of eq.(19) correlates with the τ -independent $\sim -|\varepsilon|^{-1}$ behavior leading to the $|\ln T|$ contribution in α_z . In contrast, K_2 and K_3 reduce to finite values in low T limit.

IV. DESCRIPTION OF HQV PAIR IN PDB PHASE IN LONDON LIMIT

To correctly understand the order parameter structures of a HQV pair obtained numerically, it is useful to have an intuitive image of a HQV pair by describing it in the London limit where the order parameter $A_{\mu j}$ is described in terms of the angle variables while keeping the overall amplitude fixed. Hereafter, we focus on the HQV lines extended along the polar axis \hat{z} .

First, let us review how to describe a single HQV [10]. By expressing a relative rotation around the x -axis between the orbital and spin frames in terms of the rotation matrix $(R_x(\theta))_{\mu\nu} = \hat{x}_\mu \hat{x}_\nu + \delta_{\mu\nu}^{(x)} \cos\theta - \varepsilon_{x\mu\nu} \sin\theta$, the order parameter in the PdB phase in an environment with a uniaxially stretched anisotropy is expressed following the notation in Ref.[17] as

$$\begin{aligned} A_{\mu j} &= |\Delta| e^{i\Phi} (R_x(\theta))_{\mu\nu} \left(\frac{c}{\sqrt{2}} \delta_{\nu j}^{(z)} + \sqrt{1-c^2} \hat{z}_\nu \hat{z}_j \right) \\ &= \frac{|\Delta|}{\sqrt{2}} e^{i\Phi} \begin{pmatrix} c & 0 & 0 \\ 0 & c \cos\theta & -\sqrt{2(1-c^2)} \sin\theta \\ 0 & c \sin\theta & \sqrt{2(1-c^2)} \cos\theta \end{pmatrix}, \end{aligned} \quad (20)$$

where c ($0 \leq c \leq \sqrt{2/3}$) is the parameter playing the role of the order parameter of the PdB phase, $\delta_{\mu\nu}^{(x)} = \delta_{\mu\nu} - \hat{x}_\mu \hat{x}_\nu$, and the overall phase Φ was introduced. A single HQV localized at the origin is expressed by choosing $\Phi = \theta = \phi/2$. Then, the corresponding order param-

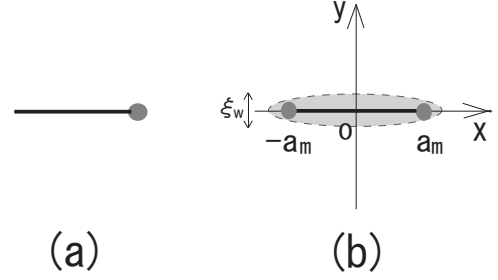


FIG. 2: (a) A single HQV (solid dot) in a B phase described in the x - y plane. To make the order parameter $A_{\mu,j}$ single-valued, its one component must vanish on the string (solid line). (b) A pair of HQVs in a B phase is accompanied by the string on which $A_{\mu,j}$ becomes the two-dimensional planar state. This planar string has the length $\simeq 2a_m$ and a width ξ_w if this HQV pair is well defined. In the double-core vortex in the bulk liquid, the string shrinks, and the planar state appears only at the center of the vortex, i.e., the origin (see sec.V).

eter becomes

$$A_{\mu j} = \frac{|\Delta|}{\sqrt{2}} \left[c e^{i\phi/2} \hat{x}_\mu \hat{x}_j + \sqrt{1 - \frac{c^2}{2}} \left(e^{i\phi} \hat{e}_{-\mu} \hat{e}'_{+j} + \hat{e}_{+\mu} \hat{e}'_{-j} \right) \right], \quad (21)$$

where the unit vectors $\hat{e}_{\pm\mu} = (\hat{y} \pm i\hat{z})_\mu / \sqrt{2}$, and $\hat{e}'_{\pm j} = (c\hat{y} \pm i\sqrt{2(1-c^2)}\hat{z})_j / \sqrt{2-c^2}$ were introduced. The fact that only A_{xx} does not become a single-valued component upon circling the vortex center implies that, as sketched in Fig.2(a), A_{xx} inevitably vanishes on a wall corresponding to a branch cut with a fixed ϕ -value. In other words, a polar-distorted *planar* phase is realized on the wall [10, 11]. The above expression of the order parameter in the London limit is easily generalized to the case with a HQV pair. Since we should consider a HQV pair to be compared with the ordinary phase vortex with an integer winding number of the phase, the angle variables Φ and θ will be chosen in the manner

$$\Phi = \frac{\phi_+ + \phi_-}{2}, \quad \theta = \frac{\phi_+ - \phi_-}{2} \quad (22)$$

where $\phi_{\pm} = \tan^{-1}[y/(x \mp a)]$. Then, eq.(21) is replaced by eq.(20) with eq.(22), i.e.,

$$\begin{aligned} A_{\mu j} &= \frac{|\Delta|}{\sqrt{2}} \left[c e^{i(\phi_+ + \phi_-)/2} \hat{x}_\mu \hat{x}_j + \sqrt{1 - \frac{c^2}{2}} \left(e^{i\phi_+} \hat{e}_{-\mu} \hat{e}'_{+j} \right. \right. \\ &\quad \left. \left. + e^{i\phi_-} \hat{e}_{+\mu} \hat{e}'_{-j} \right) \right]. \end{aligned} \quad (23)$$

In this case sketched in Fig.2(b), the expression of A_{xx} implies that the order parameter in $|x| > a$ is continuous through the x -axis, while the wall is necessary in $|x| < a$. In the polar limit where $c \rightarrow 0$, this expression reduces to the order parameter of the polar phase with the d -vector $d_\mu = \hat{z}_\mu \cos\theta - \hat{y}_\mu \sin\theta$.

Next, the dependence of the HQV pair's energy on the HQV pair size $2a$ will be considered using the gradient

energy terms. The a -dependent contribution of the vortex energy will be denoted as $\Delta F_L(a) = F(a) - F(\xi_c)$, where ξ_c is a cut off length corresponding to the core size of a HQV over which the London limit may be used. Since only the vortex lines straight along the z -axis are considered, any gradient terms including the gradient ∂_z are neglected. If our attention is paid only to such terms in the quadratic gradient energy of eq.(15), the corresponding $\Delta F_L(a)$ becomes

$$\Delta F_L^{(2)}(a) = -\frac{\pi}{2}c^2|\Delta|^2(K_1 + K_2)\ln\left(\frac{2a}{\xi_c}\right) \quad (24)$$

in clean limit where $\tau^{-1} = 0$, where $K_1 + K_2 \simeq 7\zeta(3)\xi_0^2 N(0)T_{c0}^2/(30T^2)$, and $\xi_0 = v/(2\pi T_{c0})$. The corresponding results in the two limits of eq.(24) are already known: Such an energy gain of the double-core vortex relative to the so-called o -vortex [18] in the bulk B phase is given by eq.(24) with $c^2 = 2/3$ [8, 10]. Further, the factor c^2 in eq.(24) is consistent with the vanishing $\Delta F_L^{(2)}(a)$ in the opposite polar limit where $c = 0$ [6]. It can be checked that the nonvanishing eq.(24) proportional to c^2 follows only from spatial variations of A_{xx} which is negligible in the polar phase. As shown in Ref.[6], the negative $\Delta F_L(a)$ in the polar limit occurs only from the gradient term expressing the Fermi-liquid (FL) or spin-fluctuation correction, and the corresponding contribution to $\Delta F_L(a)$ is given, in the FL model, by [6]

$$\begin{aligned} \Delta F_L^{(4)}(a) &\simeq \frac{c^{-2}}{30}\Gamma_1^s|\psi^{(2)}(1/2)|\left(\frac{T_{c0}|\Delta|}{\pi T^2}\right)^2\Delta F_L^{(2)}(a) \\ &\simeq -0.1\pi\Gamma_1^s\left(\frac{T_{c0}|\Delta|}{\pi T^2}\right)^2\xi_0^2 N(0)|\Delta|^2\ln\left(\frac{2a}{\xi_c}\right) \end{aligned} \quad (25)$$

where the next order terms of $O(c^2)$ were neglected. Here, $\psi^{(2)}(1/2) = -14\zeta(3)$, and $\Gamma_1^s = F_1^s/(1 + F_1^s/3)$ is the pressure-dependent constant of order unity with a Landau parameter $F_1^s(> 0)$. Thus, the energy gain corresponding to an attractive force in a HQV pair is dominated by the FL correction term rather than the ordinary weak-coupling terms in the strongly anisotropic PdB phase with a low enough $|c|$ -value.

In the present PdB phase, we also have an energy cost due to the planar wall. This contribution due to the nonzero A_{xx} is estimated like

$$\Delta F_w(a) \simeq 0.1N(0)\xi_0^2|\Delta|^2a/\xi(T), \quad (26)$$

where $\xi(T) = \xi_0(N(0)/|\alpha|)^{1/2}$. The coefficient $\Delta F_w(a)/a$ measures the line tension of the wall per unit length. By optimizing the sum $\Delta F_L^{(2)} + \Delta F_L^{(4)} + \Delta F_w$ w.r.t. a , the pair size to be realized is given by

$$2a_m \simeq c^{-2}\frac{2\Gamma_1^s}{\pi}\left(\frac{|\Delta|}{T}\right)^2\xi(T). \quad (27)$$

In this way, It is expected in the London limit that the size of a HQV pair, a_m , i.e., the longer radius of the elliptical core of the double-core vortex, is a microscopic scale in the bulk B phase, while, in a strongly anisotropic PdB phase close to T_{PB} where $|c| \ll 1$, the pair size may become a macroscopic one. This result will be used to explain the content of our numerical results in the next section.

If, as in the conventional GL approach [17–22], the FL corrected gradient term is neglected, the HQV pair size would remain microscopic so that the presence [7] of a macroscopic HQV pair in the PdB phase could not be explained. The appearance of a macroscopic HQV pair in the PdB phase is a combined effect of a strong anisotropy and the FL correction to the free energy.

V. NUMERICAL ANALYSIS AND RESULTS

In our numerical study, the GL model we use consists of the three free energy contributions to the free energy density, f_{bulk} and f_{grad} , defined in sec.III and the additional $O(|\Delta|^4)$ contributions $f_{\text{grad}}^{(4)}$. Before proceeding to discussing about our numerical results, comments on the $O(|\Delta|^4)$ gradient terms [6] have to be given.

Among the two terms composing $f_{\text{grad}}^{(4)}$, the stability of HQVs in the polar and A phases is determined by the contribution arising from the repulsive channel of the interaction between the quasiparticles to $f_{\text{grad}}^{(4)}$. Hereafter, to simplify our description, we will use the Fermi liquid (FL) model of such an interaction contribution to $f_{\text{grad}}^{(4)}$ for our numerical study. The corresponding gradient energy contribution $f_{\text{FL}}^{(4)}$, described in Fig.3(a), has been derived in Ref.[6] by neglecting the anisotropy effects and, in the limit of strong anisotropy, takes the form

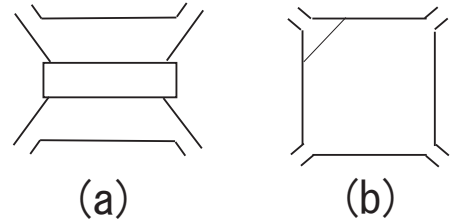


FIG. 3: (a) Diagram giving the FL-correction to the gradient energy. The rectangle denotes the vertex part representing the renormalized interaction between the quasiparticles. (b) One example of a vertex correction to the weak coupling quartic order term (Gor'kov box).

$$\begin{aligned}
f_{FL}^{(4)} = & \frac{N(0)}{450} \Gamma_1^s (\pi v)^2 \left(T \sum_{\varepsilon > 0} \frac{1}{\tilde{\varepsilon}_\infty^3} \right)^2 \left[(\nabla \cdot A_\mu) (\nabla \cdot A_\lambda^*) A_{\mu i}^* A_{\lambda i} + (\nabla A_{\mu i}) \cdot (\nabla A_{\lambda j}^*) A_{\mu i}^* A_{\lambda j} + (A_\lambda \cdot \nabla) A_{\lambda i}^* (A_\mu^* \cdot \nabla) A_{\mu i} \right. \\
& - \left((\nabla A_{\mu i}^*) \cdot (\nabla A_{\lambda j}^*) A_{\mu i} A_{\lambda j} + (A_\mu \cdot \nabla) A_{\mu i}^* (A_\lambda \cdot \nabla) A_{\lambda i}^* + (\nabla \cdot A_\mu^*) (\nabla \cdot A_\lambda^*) A_{\mu i} A_{\lambda i} \right) \\
& + 2 \left[(\nabla \cdot A_\mu) (A_{\mu i}^* (A_\lambda \cdot \nabla) A_{\lambda i}^* + A_{\lambda i} (A_\mu^* \cdot \nabla) A_{\lambda i}^*) + A_{\mu i}^* ((A_\lambda \cdot \nabla) A_{\lambda i}^* \cdot \nabla) A_{\mu i} \right. \\
& \left. - \left((\nabla \cdot A_\mu^*) (A_{\lambda i} (A_\mu \cdot \nabla) A_{\lambda i}^* + A_{\mu i} (A_\lambda \cdot \nabla) A_{\lambda i}^*) + A_{\lambda i} ((A_\mu \cdot \nabla) A_{\mu i}^* \cdot \nabla) A_{\lambda i}^* \right) \right] + \text{c.c.} \Big], \quad (28)
\end{aligned}$$

where the spin-antisymmetric Landau parameter Γ_1^a was assumed to be negligibly small [6]. The corresponding expression in the isotropic case where $\delta = 0$ is given by replacing $\tilde{\varepsilon}_\infty$ in eq.(28) by $\tilde{\varepsilon}_0$. Although eq.(28) does not include the anisotropy parameter δ explicitly, the anisotropy-induced vertex correction with $C_0 - 1$ as a coefficient is, as is explained in Appendix, safely negligible even in the limit of strong anisotropy.

Another contribution to $f_{\text{grad}}^{(4)}$ arises from the ordinary weak-coupling $O(|\Delta|^4)$ term, the so-called "Gor'kov box", unaccompanied by a repulsive interaction between quasiparticles (see Fig.3(b)). This contribution includes all the terms including those expressed by C_{21} , B_0 , and ΔB , in the vertex correction Λ_j . As is explained in relation to Fig.7(a), however, these vertex corrections are also safely negligible. This has been concluded through the full numerical results, although it is already known [6] that these anisotropy-induced terms unaffected the resulting size of the HQV pair irrespective of the anisotropy value. Therefore, regarding $f_{\text{grad}}^{(4)}$ to be added to f_{bulk} and f_{grad} , its expression in the isotropic case, i.e., eq.(52) in Ref.[6] has been used to obtain numerical results even in the case with a strong enough anisotropy.

To numerically examine how the double-core vortex becomes stable as a HQV pair, we follow the previous work on the double-core vortex in the B phase in the isotropic aerogel [8]: First, eq.(23) is used as the initial condition for searching a half-core pair with the lowest energy at fixed values of the temperature and pressure. This London solution, eq.(23), has a fixed size $2a$ of the HQV pair as a parameter. Alternatively, the texture of the order parameter at the outer boundary is initially set by a fixed a -value. The variational equations of the GL free energy explained above are solved to obtain the solution minimizing the energy for each a -value according to the direct two-dimensional method [19], i.e., by assuming the vortices to be straight line objects extending along the z -axis. During this procedure, we have checked that the size of the half-core pair of the *resulting* double-core vortex solution surely coincides with the $2a$ value at the initial condition. Thus, in examining the dependence of the vortex energy

$$\Delta F(a) = F(a) - F(0) \quad (29)$$

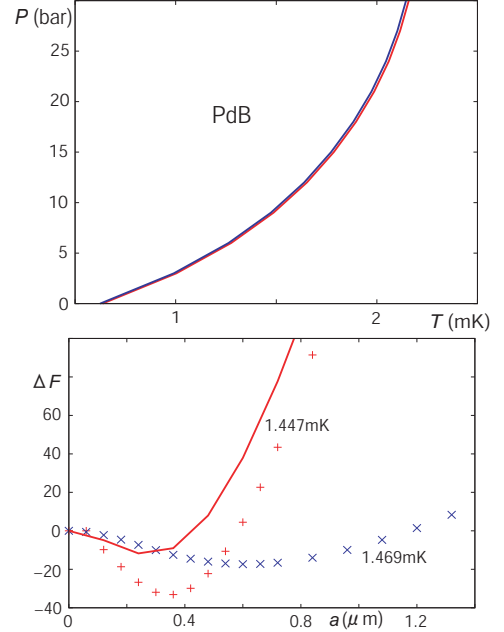


FIG. 4: Numerical results for $\delta = 0.05$. (a) P v.s. T phase diagram. The red solid curve is the superfluid transition curve $T_c(P)$ between the polar and normal phases, while the blue one is $T_{PB}(P)$ and is quite close to $T_c(P)$. (b) The a v.s. $\Delta F(a)$ curves at $P = 9$ (bar) and at $T = 1.447$ (red plus symbols) and 1.469 (blue cross symbols) (mK). The a -value, a_m , minimizing $\Delta F(a)$ in each case is given in Table I to be given later. For comparison, the corresponding curve at 1.447(mK) in the case with no FL correction is shown by the solid red curve which indicate $a_m = 0.24(\mu\text{m})$.

on the a -value introduced as the initial condition below, this a can be identified with the half of the resulting size of the half-core pair. Here, $\Delta F(a)$ corresponds to $\Delta F_L(a)$ introduced in the London limit. In the language of the vortices in the bulk B phase, the $F(0)$ corresponds to the free energy of the so-called o -vortex [18].

In our computations studying the vortices extending along the z -axis, the system size in the x (y) direction was fixed to 24 (1.2) (μm) in the layout sketched in Fig.2(b). The pressure dependence of the system is incorporated through that of the bulk transition temperature T_{c0} and

the Fermi velocity v [21]. The dimensionless strength of the impurity scattering is $(\tau T_{c0})^{-1}$ which is enhanced with decreasing the pressure reflecting the pressure dependence of T_{c0} [8, 22].

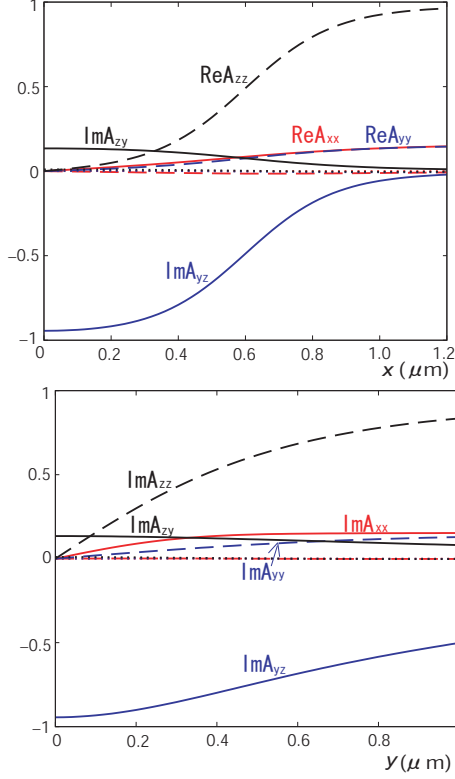


FIG. 5: Spatial variations of $A_{\mu j}$ components for $\delta = 0.05$ on sweeping (a) along the x -axis and at $y = 0$ at $a_m \simeq 0.6(\mu\text{m})$ when $T = 1.469(\text{mK})$ and $P = 9(\text{bar})$ and (b) along the y -axis and at $x = 0$. Here, the vortex center is at $(0, 0)$. The $A_{\mu j}$ components other than the nonvanishing five components in the London representation, eq.(20), are expressed by the dotted curves and a red dashed curve.

Throughout the present study, the dipole energy is not taken into account. The neglect of the dipole energy is justified in the case of weaker anisotropy where the resulting size of the half-core pair is much smaller than the dipole length $\xi_D \sim 10(\mu\text{m})$. In contrast, a HQV pair resulting from a strong enough anisotropy may have a size of the order of ξ_D over which the dipole energy affects spatial patterns of the θ -variable, defined in eq.(20), in the PdB phase [7]. However, one will see below in this section that the London limit becomes a better description as a HQV pair typically grows accompanying the increase of the anisotropy. Then, the dipole energy has only to be taken into account in a description starting from the London limit [7].

Hereafter, as our numerical results at some δ -values, we

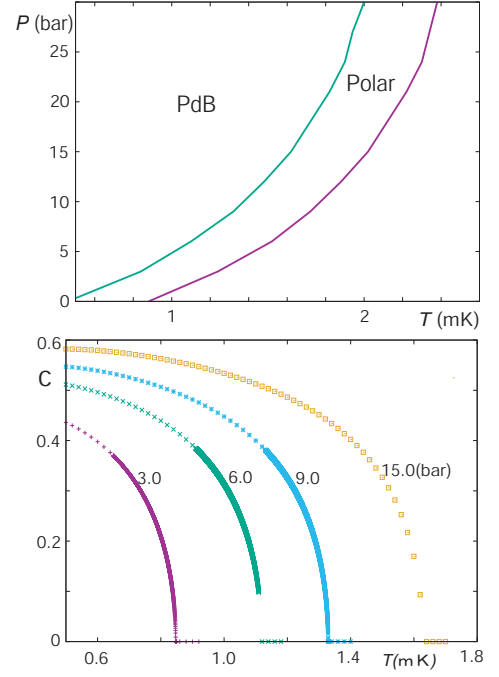


FIG. 6: Numerical results for $\delta = 4.4$. The pressure P v.s. temperature T phase diagram (a) in which the blue curve is the superfluid transition curve $T_c(P)$ between the polar and normal phases, and the red one is $T_{PB}(P)$. The figure (b) shows the temperature dependence of the "order parameter" c in the PdB phase at the pressures $P = 3.0$ (bottom), 6.0 , 9.0 , and 15.0 (top) (bar).

will present $\Delta F(a)$ data and x and y dependences of each component of the order parameter $A_{\mu,j}$ of the vortex solution minimizing $\Delta F(a)$. The τ^{-1} -value will be fixed to $0.13(\text{mK})$ hereafter. First, the $\delta = 0.05$ case is discussed as a typical example of superfluid ^3He in a *weakly anisotropic* aerogel. Figure 4 (a) and (b) express the corresponding phase diagram and the a v.s. $\Delta F(a)$ curves at $T = 1.469(\text{mK})$ close to T_{PB} and $1.447(\text{mK})$ at a fixed pressure $P = 9(\text{bar})$, while Fig.5(a) and (b) present spatial variations of each component of $A_{\mu,j}$ on sweeping along the x and y axis, respectively. Here, the HQV pair is always assumed to be initially set as in Fig.2(b), and the origin is the center of the HQV pair. Further, by symmetry, just the region in $x \geq 0$ and $y \geq 0$ is shown.

As Fig.4(a) shows, the polar phase region in this $\delta = 0.05$ case is extremely narrow, and T_{PB} and T_c curves are quite close to each other. In Fig.4(b), the dependence of the vortex core energy ΔF on the initial value $2a$ of the half-core pair size is presented for the two values of $c(T)$. As Fig.6(b) shows, the parameter c playing the role of the order parameter in the PdB phase grows upon cooling. The $2a$ value minimizing ΔF corresponds to the half-core pair size $2a_m$ to be realized. Closer to the phase boundary T_{PB} at which c vanishes, the a_m value becomes larger as suggested by eq.(27). Further, as the solid curve in Fig.4(b) shows, the conventional GL free energy with no FL correction term eq.(28) results in a smaller size

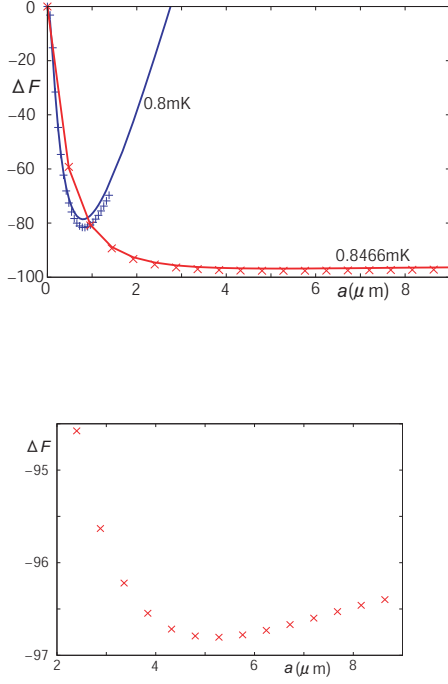


FIG. 7: Numerical results for $\delta = 4.4$ at 3(bar). In the figure (a), the a v.s. $\Delta F(a)$ curves are expressed by the blue symbols at 0.8(mK) and by the red symbols at 0.8466(mK) close to T_{PB} , and they have $a_m = 0.84 (\mu\text{m})$ and $a_m = 5.28 (\mu\text{m})$, respectively. For comparison, the results (solid curves) in the case with additional vertex corrections (see the text) are also shown. The figure (b) is the extended view of the red symbols around $a = 5.28$ in (a).

$2a_m = 0.48(\mu\text{m})$ of the half-core pair [8, 23]. Such a correlation-induced growth of the half-core pair size has also been pointed out elsewhere [8, 23]

Figure 5 (a) and (b) show spatial variations of $A_{\mu,j}$ on sweeping along the x and y axis, respectively, for $c = 0.2$ and $\delta = 0.05$. Broadly speaking, the midpoint of A_{yz} and A_{zz} curves correspond to the position of the half-core, i.e., $x = a_m$. In the isotropic case where $c^2 = 2/3$ irrespective of the temperature, $|A_{yz}|$ and $|A_{zz}|$ at the origin coincide with each other. A large difference between them at $x = 0$ appears in Fig.4(b) due to the "anisotropy" value, $c = 0.2$. This can be understood from eq.(20) with $\phi_+ = \pi$ and $\phi_- = 0$. On approaching the vortex center along the x -axis, A_{xx} decreases. Nevertheless, A_{xx} seems to be nonvanishing even close to $x = 0$. It means that the planar state is realized only in the close vicinity of the origin. Further, the width ξ_w defined in Fig.2(b), i.e., range of y over which A_{xx} linearly decreases is large ($\simeq 0.3$) as Fig.5(b) shows. These behaviors of A_{xx} imply that, in spite of a substantial size $2a_m$ of the half-core pair (see Table 1), the planar string (wall) expected in the London description in sec.III is ill-defined when $\delta = 0.05$. In fact, the a -dependence of $\Delta F(a)$ in $a > a_m$ in Fig.4(b) seems to be different from the expected linear behavior in a . Therefore, the half-core structure of the double-core vortex cannot be

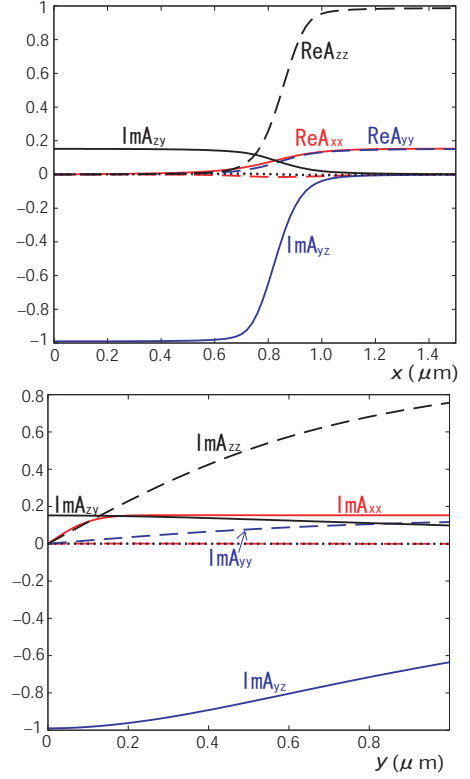


FIG. 8: The figure (a) expresses the data, at $a = a_m = 0.84$ of the blue symbols in Fig.7(a), of spatial variations of $A_{\mu,j}$ components on sweeping along the x -axis and at $y = 0$. The figure (b) corresponds to (a) on sweeping y and at $x = 0$. Here, the vortex center is at $(0, 0)$.

identified with a HQV pair in the case of low anisotropy such that $\delta = 0.05$.

Next, the corresponding results in a case with a moderately strong anisotropy, $\delta = 4.4$, are presented in Figs.6 and 7. The P - T phase diagram and the temperature dependence of the order parameter c of the PdB phase are given in Fig.6(a) and (b), respectively. Figure 6(a) shows that a moderately wide region of the polar phase is realized in this case. As pointed out elsewhere [15, 16, 24], the superfluid transition (right solid) curve is not changed notably depending on the "impurity" strength τ^{-1} , while the $T_{PB}(P)$ (left solid) curve is sensitive to τ^{-1} , and a slight increase of τ^{-1} remarkably broadens the polar phase region. In Fig.7(a) and Fig.8, we focus on the $P = 3(\text{bar})$ case and on the results at the two temperatures, 0.8466(mK) at which $c = 0.0456$ and 0.8(mK) at which $c = 0.214$.

Figure 8(a) and (b) express the spatial variations of the components of $A_{\mu,j}$ at 0.8 (mK) in $P = 3(\text{bar})$ when $\delta = 4.4$ and correspond to Fig.5(a) and (b). Some clear differences between Fig.8(a) and Fig.5(a) are seen. First, in the notation of eq.(23), the following relations are satisfied in Fig.8(a); $\theta \simeq 0$ and $|A_{xx}| \simeq c/\sqrt{2}$ in $x > a_m$, while $\theta \simeq \pi/2$ and $|A_{xx}| = 0$ in $0 \leq x < a_m$. Next, the linearly vanishing behavior of A_{xx} (red solid curve)

on lowering $|y|$ and at $x = 0$ is seen only in a narrow region near the origin so that $\xi_w \simeq 0.1(\mu\text{m})$. In addition, the linear behavior $\Delta F(a) \propto a$ is nicely seen in $a > a_m$ in Fig.7 (a) and (b), implying that the planar string is well-defined and has a length comparable with the size $2a_m$ of the half-core pair. In fact, Fig.7 (a) and (b) shows that such a linear behavior approximately obeys the relation $f(T)c^2a$ where the T -dependent coefficient $f(T)$ slowly increases upon cooling, i.e., a relation consistent with the London result eq.(26). Further, except in the vicinity of the half-core, other components of $A_{\mu,j}$ than the five nonvanishing ones in eq.(20) can be regarded as being zero.

Based on these features, in contrast to the $\delta = 0.05$ case, the double-core vortex in $\delta = 4.4$ is consistent with the description in London limit and can be well regarded as a HQV pair. However, the origin of this consistency with eq.(23) cannot be ascribed merely to the growth of the half-core pair. For instance, the anisotropic growth of the double vortex core also may occur due to an enhanced rigidity. In such a situation expected to occur in *isotropic* aerogel [8], the growth of the half-core pair is accompanied by the corresponding *enhancement* of the components of $A_{\mu,j}$ which are zero in eq.(20) [8], contrary to the feature seen in Fig.8(a) and (b). The reason why the double core vortex in the PdB phase in such a moderately strong anisotropic case is well described by the London limit seems to consist in the simple structure of the HQV in the $c \rightarrow 0$ limit, i.e., in the polar phase. As shown in Ref.[6], the spatial variations of the order parameter are surprisingly simple and are well represented by eq.(23) with $c = 0$ and $A_{xx} = 0$ except in the close vicinity of each HQV. A smaller c -value effectively implying a stronger anisotropy leads to a structure closer to that in the London limit.

Further, in Fig.7(a), we have also presented the $\Delta F(a)$ v.s. a curves (solid curves) in the case where the $O(|\Delta|^4)$ gradient energy includes all of the vertex corrections accompanied by C , B , and D in eq.(7). The deviation from the case (crossed symbols) with no such vertex corrections in the $O(|\Delta|^4)$ gradient energy is negligibly small, and the resulting a_m value remains unchanged by including such vertex corrections. Therefore, we judge that the neglect of the vertex corrections to the $O(|\Delta|^4)$ gradient terms, mentioned in the beginning of this section, is valid in all of other results presented here.

Figure 9 (a) and (b) express spatial variations of $A_{\mu,j}$ for a much stronger anisotropy, $\delta = 300$, and correspond to Fig.8 (a) and (b) for $\delta = 4.4$. Surprisingly, the two sets of the figures are qualitatively similar to each other, suggesting that the $\delta = 4.4$ case already enters the limit of the strong anisotropy. In fact, the size a_m of the HQV pair minimizing the energy at the same c -value depends weakly on the anisotropy δ and, as Table 1 shows, takes quite similar values between the two cases with quite different δ values.

Next, the P (pressure) and c dependences of the a_m value presented in Table 1 will be discussed. The results

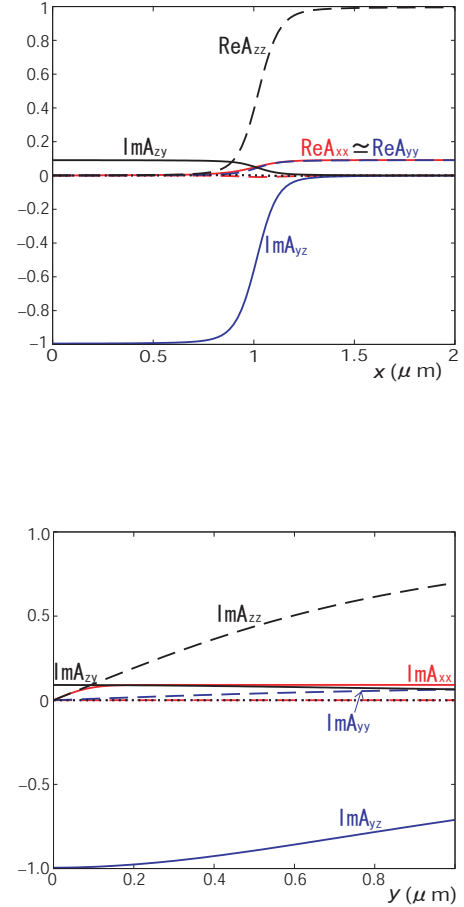


FIG. 9: Spatial variations of $A_{\mu,j}$ at 0.55(mK) below T_{PB} , where $c = 0.217$, at 3(bar) for $\delta = 300$ obtained on sweeping (a) along the x axis and (b) along the y axis, respectively.

in $P = 3$ (bar) and 9 (bar) at a fixed c value indicate that the resulting a_m becomes smaller with increasing P . However, it should be noted that, under a fixed c value, an increase of P corresponds to a higher temperature according to Fig.6(b), and that, as eq.(27) suggests, a_m increase upon cooling. That is, the pressure dependence of a_m at a fixed c listed in Table I may be understood based, at least in part, on its T dependence. Further, by taking account of the T -dependence eq.(27) suggests, one finds that the a_m value under a similar c value is not sensitive much to the anisotropy δ . This is consistent with the viewpoint mentioned above that the system with $\delta = 4.4$ is already in the regime of the strong anisotropy.

On the other hand, the c dependence of a_m is not fully understood based on the London limit. In fact, the c dependence of a_m is much weaker than that suggested by eq.(27), and the a_m value increases only weakly with

δ	0.05	0.05	4.4	4.4	4.4	300	300
$P(\text{bar})$	9	9	9	3	3	3	3
$T(\text{mK})$	1.447	1.469	1.28	0.8	0.8466	0.55	0.6396
c	0.5	0.2	0.219	0.214	0.046	0.217	0.055
$a_m(\mu\text{m})$	0.36	0.6	0.54	0.84	5.28	0.82	6.24

TABLE I: Resulting a_m values at different temperatures for various δ -values at 3 and 9(bar). The c -value in each case is also shown.

vanishing c . Judging from the fact that the linear a behavior of ΔF is seen in Fig.7 (b), this discrepancy does not seem to be due to the smallness of the system size. On the other hand, the logarithmic behavior of eq.(25), which has been nicely verified in the polar phase [6], is masked in the present case by the linear behavior eq.(27). Hence, we cannot clarify whether the contribution corresponding to eq.(25) is satisfied or not in the present case.

VI. SUMMARY

In this work, we have numerically examined the stability of a HQV pair in the PdB phase of the superfluid ^3He

δ	0.05	0.05	4.4	4.4	4.4	4.4	300	300
$P(\text{bar})$	9	9	9	9	3	3	3	3
$T(\text{mK})$	1.447	1.469	1.28	1.33	0.8	0.8466	0.55	0.6396
c	0.5	0.2	0.219	0.0327	0.214	0.046	0.217	0.055
$\xi_w(\mu\text{m})$	0.2	0.286	0.073	0.121	0.105	0.226	0.092	0.299

TABLE II: Resulting thickness of the Kibble (planar) wall obtained based on the definition given in the text at different temperatures for various δ -values at 3 and 9(bar).

Here, the present result will be compared with the experimental result in Ref.[7], where the HQV pairs in the PdB phase have been detected. First, the width of the planar string ξ_w is expected by comparing the mass term and the gradient one of $O(A_{xx}^2)$ with each other to be roughly estimated as $\xi(T)/c$ [7, 10]. From the numerical data, ξ_w will be defined by assuming that the y dependence of A_{xx} close to the origin is approximated by $c \tanh(y/\xi_w)/\sqrt{2}$ [7] (see also eq.(20)). As Table II shows, ξ_w indeed grows with decreasing c , though the c dependence is apparently weaker compared with the relation mentioned above. The deviation from the c^{-1} dependence seems to be resolved by noting that both c and $\xi(T)$ are T -dependent. On the other hand, the δ dependence of ξ_w is not anticipated easily and is found only through the present numerical analysis. Table II suggests that, with increasing δ , the aspect ratio $2a_m/\xi_w$ becomes large enough to make the planar string a rigid

in a strongly anisotropic aerogel by assuming the weak coupling approximation and based on the hypothesis that the double-core vortex in the bulk B phase corresponds to the HQV pair in the PdB phase. Due to the weak coupling approximation, the presence of the PdA phase in real systems is neglected, and the transition between the PdB and the polar phases becomes inevitably continuous in the present analysis. However, such a continuous transition is found at low enough pressures in real systems [25], and in this sense the present results may be directly applicable to the experimental situations.

Our main result in the present work is that the double-core vortex [19, 20] in the PdB phase under a strong anisotropy can be regarded as a HQV pair described in the London limit. This is a reflection of the fact that the HQV in the pure polar phase is well described in the London limit [6].

and well defined object. Note that this ratio is inversely proportional to c , reflecting the proximity to the polar phase in which the HQV pair is infinitely long with no dipole energy neglected in the present analysis. Broadly speaking, an anisotropy value δ larger than unity is necessary for the double-core vortex to become a well-defined HQV-pair, and, as also indicated in sec.V, the case with $\delta = 4.4$ belongs to the case of infinitely large anisotropy, judging from the fact that the a_m and ξ_w values under a similar c -value do not change much between the $\delta = 4.4$ and 300 cases. On the other hand, the c dependences of a_m and ξ_w are seemingly in disagreement with the expectation based on the London limit. It is unclear whether this discrepancy can be fully resolved by taking account of the T and P dependences of the coefficients in the GL free energy.

The results on the vortex energy shown in Figs.4 and 7 imply together with the data in Table I that the size

of the HQV pair, a_m , is highly sensitive to the c -value. On the other hand, huge HQV pairs in the PdB phase have appeared in Ref.[7] in spite of a reasonable T dependence of c corresponding to $\sqrt{2}q$ there (see Supplementary Fig.5 in Ref.[7] which is qualitatively comparable with Fig.6(b)). It is an evidence of the presence of a strong pinning effect in real systems supporting the huge HQV pair in the nematic aerogels [7].

In the experiment under rotation [1], the rotation axis has been fixed to the anisotropy (polar) axis, which is the z -direction in our notation. Further, as mentioned above, the vortices created under a rapid quench [7] are also pinned along the polar axis because the mean free path for the quasiparticles is the longest in this direction. Thus, it is possible that, if rotating the aerogel with a rotation axis perpendicular to the polar axis, a pinning of the resulting vortices to the aerogel structure may be avoided. Then, the shrinkage of the HQV pair upon cooling might be observed in such a situation. There is another motivation regarding a study of HQVs extending along a direction perpendicular to the polar axis. Recently, NMR measurements for ^3He in a nematic aerogel squeezed by 30 percent in a direction perpendicular to the polar axis have been reported [24]. There, it has been found that the l -vector in the chiral PdA phase is largely directed along the squeezed direction. In this situation, the Majorana fermions may remain stable [26] in the core of a HQV in the PdA phase. For these reasons,

it will be valuable to extend the present study on HQVs to the situation with the vortex axis perpendicular to the polar axis.

VII. APPENDIX A

In this Appendix, details of the pairing vertex correction due to the impurity scattering and of the coefficient of each term in the resulting GL free energy are explained.

The impurity scattering potential does not carry the Matsubara frequency, and consequently, the corresponding self energy term can be incorporated through the replacement of the Matsubara frequency $|\varepsilon|$ with

$$\begin{aligned} |\tilde{\varepsilon}_p| &= |\varepsilon| + \frac{1}{2\tau} \langle w(p - p') \rangle_{p'} \\ &= |\varepsilon| + \frac{1 + (\delta^{-1/2} - 1)\theta(1 - \delta)}{4\tau} (\tan^{-1}(\delta^{1/2}(1 - p)) \\ &\quad + \tan^{-1}(\delta^{1/2}(1 + p))) \end{aligned} \quad (30)$$

($|p| < 1$), where $p = \mathbf{p} \cdot \hat{z}/p_F$, $\langle \rangle_p$ implies the average over the polar angle $\cos^{-1}(p)$.

The coefficients composing the vertex part Λ are given in the form

$$\begin{pmatrix} B_0 & D_0 \\ \Delta B & \Delta D \end{pmatrix} = \frac{1}{2} \begin{pmatrix} 1 - I_{d11} & -\delta^{-1}(I_{d10} - I_{d11}) \\ -\delta(3I_{d12} - 4I_{d13}) & 1 - 3I_{d11} + 7I_{d12} - 4I_{d13} \end{pmatrix}^{-1} \begin{pmatrix} e_1 & -I_{d21} + 2\delta^{-1}C_0(I_{d20} - I_{d21}) - e_1 \\ e_2 & 2C_0(3I_{d21} - 7I_{d22} + 4I_{d23}) - e_2 \end{pmatrix} \quad (31)$$

where

$$e_1 = I_{d21} + \delta^{-1}(I_{d21} - I_{d20}), \quad (32)$$

$$\begin{aligned} e_2 &= \delta(3I_{d22} - 4I_{d23}) \\ &\quad - 3I_{d21} + 7I_{d22} - 4I_{d23}, \end{aligned} \quad (33)$$

and

$$\begin{aligned} C_0 &= \frac{1}{d}, \\ C_{21} &= \frac{-I_{d31} + I_{d32} + \delta^{-1}(I_{d30} - 2I_{d31} + I_{d32})}{d^2}, \\ C_{1z} &= 2dC_{21} - \frac{2}{d}(B_0(I_{d21} - I_{d22}) \\ &\quad + \Delta B(I_{d20} - 2I_{d21} + I_{d22})), \end{aligned} \quad (34)$$

$$\begin{aligned} C_{2z} &= \frac{1}{d}((2 + C_0)(I_{d31} - I_{d32}) - 2D_0(I_{d21} - I_{d22})) \\ &\quad - \frac{1}{d\delta}((2 + 3C_0)(I_{d30} - 2I_{d31} + I_{d32}) \\ &\quad + 2\Delta D(I_{d20} - 2I_{d21} + I_{d22})). \end{aligned} \quad (35)$$

Further,

$$\begin{aligned} d &= 1 - 2(I_{d11} - I_{d12}), \\ I_{dmn} &= \left\langle \frac{1 + (\sqrt{\delta} - 1)\theta(\delta - 1)}{(2|\tilde{\varepsilon}_p|^m \tau (1 + \delta p^2)^n)} \right\rangle_p. \end{aligned} \quad (36)$$

Among these coefficients, the $|\varepsilon|$ dependences of $C_0 - 1$ and B_0 are presented in Fig.10(a) and (b), respectively. Here, $f = XC_0$, $g = \pi XB_0/\tau$, and $X = 4\tau|\varepsilon|/\pi$. Broadly speaking, the functions f and g decrease for smaller δ -values. Since, more or less, we focus on the temperature range in which $2\tau|\varepsilon| \gg 1$, any impurity-induced vertex corrections become negligible in our numerical analysis.

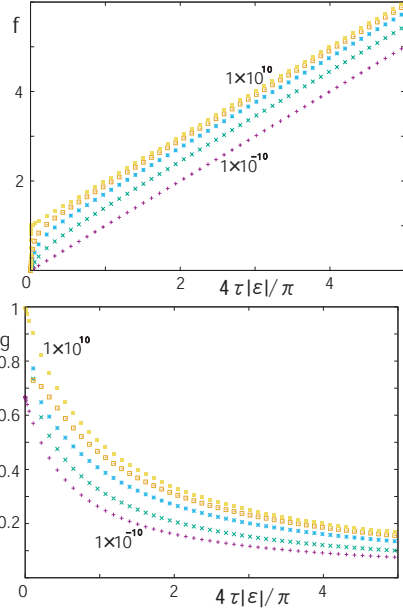


FIG. 10: (a) $f \equiv XC_0$ v.s. X curves for $\delta = 1 \times 10^{10}$ (top), 300, 30, 4.4, and 1×10^{-10} (bottom), where $X = 4\tau|\varepsilon|/\pi$. Note that f obeys $1 + X$ in $\delta \rightarrow \infty$, while it approaches X in $\delta \rightarrow 0$ limit. (b) $g \equiv \pi XB_0/\tau$ v.s. X curves corresponding to those in (a). In $\delta \rightarrow \infty$, g obeys $1/(1+X)$, while it approaches $2/[3(1 + \pi X/2)]$ in $\delta \rightarrow 0$ in agreement with eq.(9).

Next, the coefficients in the GL free energy are given by

$$\alpha = \frac{1}{3}N(0) \left[\ln\left(\frac{T}{T_{c0}}\right) + 2\pi T \sum_{\varepsilon>0} \left(\frac{1}{|\varepsilon|} - \frac{3}{2}(I_{10} - I_{11}) \right) \right],$$

$$\alpha_z = \frac{1}{3}N(0) \left[\ln\left(\frac{T}{T_{c0}}\right) + 2\pi T \sum_{\varepsilon>0} \left(\frac{1}{|\varepsilon|} - 3I_{11}C_0 \right) \right], \quad (37)$$

where

$$I_{mn} = \left\langle \frac{p^{2n}}{|\tilde{\varepsilon}_p|^m} \right\rangle_p, \quad (38)$$

$$\begin{aligned} \beta_3^{(0)} &= -2\beta_1^{(0)} = \frac{\pi T}{8}N(0) \sum_{\varepsilon>0} (I_{30} - 2I_{31} + I_{32}), \\ \beta_2^{(0)} &= \beta_4^{(0)} = -\beta_5^{(0)} = \beta_3^{(0)} - \frac{\pi T}{64\tau}N(0) \\ &\quad \times \int_{-1}^1 dp_1 \int_{-1}^1 dp_2 \sum_{\varepsilon>0} \frac{(1-p_1^2)(1-p_2^2)}{\tilde{\varepsilon}_{p_1}^2 \tilde{\varepsilon}_{p_2}^2 (1+\delta(p_1-p_2)^2)} (1 + (\sqrt{\delta}-1)\theta(\delta-1)), \\ \beta_z &= -\frac{3}{2}(\beta_3^{(0)} + 2\beta_3^{(1)}) + \frac{\pi T}{2}N(0) \sum_{\varepsilon>0} C_0^4 I_{32} - \frac{\pi T}{64\tau}N(0) \\ &\quad \times \int_{-1}^1 dp_1 \int_{-1}^1 dp_2 \sum_{\varepsilon>0} \frac{(1-p_1^2-2p_1^2C_0^2)(1-p_2^2-2p_2^2C_0^2)}{\tilde{\varepsilon}_{p_1}^2 \tilde{\varepsilon}_{p_2}^2 (1+\delta(p_1-p_2)^2)} (1 + (\sqrt{\delta}-1)\theta(\delta-1)), \\ \beta_3^{(1)} &= -2\beta_1^{(1)} = -\beta_3^{(0)} + \frac{\pi T}{2}N(0) \sum_{\varepsilon>0} C_0^2 (I_{31} - I_{32}), \\ \beta_2^{(1)} &= \beta_4^{(1)} = -\beta_5^{(1)} = \beta_3^{(1)} + \frac{\pi T}{64\tau}N(0) \\ &\quad \times \int_{-1}^1 dp_1 \int_{-1}^1 dp_2 \sum_{\varepsilon>0} \frac{(1-p_1^2)(1-p_2^2-2p_2^2C_0^2)}{\tilde{\varepsilon}_{p_1}^2 \tilde{\varepsilon}_{p_2}^2 (1+\delta(p_1-p_2)^2)} (1 + (\sqrt{\delta}-1)\theta(\delta-1)), \end{aligned} \quad (39)$$

$$K_2 = \frac{\pi T v^2}{16}N(0) \sum_{\varepsilon>0} (I_{32} - 2I_{31} + I_{30}), \quad (40)$$

$$K_3 = \frac{\pi T v^2}{16}N(0) \sum_{\varepsilon>0} (-5I_{32} + 6I_{31} - I_{30}), \quad (41)$$

$$K_1 = K_2 + \frac{\pi T v^2}{4} N(0) \sum_{\varepsilon > 0} [(I_{20} - I_{21})B_0 + (I_{21} - I_{22})\Delta B], \quad (42)$$

$$K_4 = -K_2 + \frac{\pi T v^2}{4} N(0) \sum_{\varepsilon > 0} [(I_{31} - I_{32})C_0 - 8I_{11}C_{21}], \quad (43)$$

$$\begin{aligned} K_5 &= 2K_3 + \frac{\pi T v^2}{8} N(0) \sum_{\varepsilon > 0} [(3I_{21} - I_{20})B_0 + (3I_{22} - I_{21})\Delta B \\ &\quad + (I_{20} - I_{21})D_0 + (I_{21} - I_{22})\Delta D + 2(I_{31} - I_{32})(C_0 - 1) \\ &\quad - 8I_{11}C_{1z}], \\ K_6 &= -7K_3 + \frac{\pi T v^2}{4} N(0) \sum_{\varepsilon > 0} [(3I_{21} - I_{20})D_0 \\ &\quad + (3I_{22} - I_{21})\Delta D + (5I_{32} - 3I_{31})(C_0 - 1) - 8I_{11}C_{2z} \\ &\quad + 3I_{31} - I_{30}]. \end{aligned}$$

VIII. APPENDIX B

Here, possible effects of the pairing vertex correction, peculiar to the anisotropic scattering, on the $O(|\Delta|^4)$ gradient energy arising from the Fermi liquid repulsive interaction will be discussed. In our previous work [6], such a vertex correction was not taken into account there by assuming a weak anisotropy.

Since, in the present work, only a straight vortex line extending along \hat{z} is considered, the gradient does not have to include its z -component ∂_z in the gradient terms. Then, the only vertex correction in the FL-corrected gradient terms is the factor $C_0 - 1$ accompanying $A_{\rho z}$ in eq.(28). For instance, the terms including $A_{\mu z}$ in the first line of eq.(28) have to be replaced by

$$\begin{aligned} &= \frac{N(0)}{225} \Gamma_1^s (\pi v_F)^2 \left[\left(T \sum_{\varepsilon > 0} \frac{1}{\varepsilon^3} C_0 \right)^2 \left[(\nabla \cdot A_\mu) (\nabla \cdot A_\lambda^*) A_{\mu z}^* A_{\lambda z} + (A_\lambda \cdot \nabla) A_{\lambda z}^* (A_\mu^* \cdot \nabla) A_{\mu z} \right] \right. \\ &\quad + \left(T \sum_{\varepsilon > 0} \frac{1}{\varepsilon^3} \right) \left(T \sum_{\varepsilon > 0} \frac{1}{\varepsilon^3} C_0^2 \right) \left[\sum_{j=x,y} (\nabla A_{\mu z}) \cdot (\nabla A_{\lambda j}^*) A_{\mu z}^* A_{\lambda j} + \text{c.c.} \right] \\ &\quad \left. + \left(T \sum_{\varepsilon > 0} \frac{1}{\varepsilon^3} C_0^2 \right)^2 (\nabla A_{\mu z}) \cdot (\nabla A_{\lambda z}^*) A_{\mu z}^* A_{\lambda z} \right]. \quad (45) \end{aligned}$$

As can be seen in Fig.10, however, $C_0(\varepsilon) - 1$ remains almost zero irrespective of the δ -value except at low enough values of $2\pi T\tau$ and is quantitatively negligible in the temperature region where $2\pi T\tau \gg 1$ is satisfied. Therefore, we can proceed our analysis without incorporating the impurity-induced vertex correction to the pairing process in the FL gradient term even in the limit of strong anisotropy.

In another gradient terms stemming from the "Gor'kov box", i.e, the ordinary weak-coupling $O(|\Delta|^4)$ term unaccompanied by a repulsive interaction between quasi-particles, the vertex corrections other than $C_0 - 1$ are

also present. As shown in sec.V of Ref.[6], this weak-coupling diagram does not contribute to the stability of HQVs in the polar and A phases irrespective of how the gradients operate onto the order parameter fields. Further, as explained in relation to Fig.7, the weak coupling $O(|\Delta|^4)$ term plays only negligible roles for the stability of a HQV-pair occurring in the B phase.

One of the authors (R.I.) is grateful to Vladimir Dmitriev and Bill Halperin for useful discussions. The present work was supported by JSPS KAKENHI (Grant No.16K05444).

-
- [1] S. Autti, V. V. Dmitriev, J. T. Makinen, A. A. Soldatov, G. E. Volovik, A. N. Yudin, V. V. Zavjalov, V. B. Eltsov, Phys. Rev. Lett. **117**, 255301 (2016).
 - [2] K. Aoyama and R. Ikeda, Phys. Rev. B **73**, 060504(R) (2006).
 - [3] V. V. Dmitriev, A. A. Senin, A. A. Soldatov, and A. N. Yudin, Phys. Rev. Lett. **115**, 165304 (2015).
 - [4] G. E. Volovik and V. P. Mineev, JETP Lett. **24**, 561

- (1976).
- [5] M. M. Salomaa and G. E. Volovik, Phys. Rev. Lett. **55**, 1184 (1985).
- [6] N. Nagamura and R. Ikeda, Phys. Rev. B **98**, 094524 (2018).
- [7] J. T. Makinen, V. V. Dmitriev, J. Nissinen, J. Rysti, G. E. Volovik, A. N. Yudin, K. Zhang, V. B. Eltsov, Nature Communication **10**, 237 (2019).

- [8] N. Nagamura and R. Ikeda, arXiv:1905.02569.
- [9] V.V. Dmitriev, A.A.Soldatov, and A.N.Yudin, Phys. Rev. Lett. **120**, 075301 (2018).
- [10] G. E. Volovik, JETP Lett. **52**, 358 (1990).
- [11] G. E. Volovik, JETP Lett. **109**, 499 (2019).
- [12] I. A. Fomin, JETP **127**, 933 (2018).
- [13] P. W. Anderson, J. Phys. Chem. Sol. **11**, 26 (1959).
- [14] N. R. Werthamer, in *Superconductivity* Vol.1 (ed. by R. D. Parks, Taylor and Francis, 1968).
- [15] V. B. Eltsov, T. Kamppinen, J. Rysti, and G. E. Volovik, arXiv:1908.01645.
- [16] R. Ikeda and M. Tange, arXiv:1908.10712.
- [17] S. Yang and R. Ikeda, J. Phys. Soc. Jpn. **83**, 084602 (2014).
- [18] T. Ohmi, T. Tsuneto, and T. Fujita, Prog.Theor.Phys. **70**, 647 (1983).
- [19] E. V. Thuneberg, Phys. Rev. B **36**, 3583 (1987).
- [20] M. M. Salomma and G. E. Volovik, Rev. Mod. Phys. **59**, 533 (1987).
- [21] D. Volhardt and P. Wolffe, "The Super uid Phases of Helium 3" (Taylor and Francis, 2002).
- [22] E.V. Thuneberg, S. K. Yip, M. Fogelstrom, and J. A. Sauls, Phys. Rev. Lett. **80**, 2861 (1998).
- [23] M. A. Silaev, E. V. Thuneberg, and M. Fogelstrom, Phys. Rev. Lett. **115**, 235301 (2015).
- [24] V. V. Dmitriev, M. S. Kutuzov, A. A. Soldatov, A. N. Yudin, arXiv:1911.01193.
- [25] J. Rystia, A.N. Yudinb, J. T. Makinen, V.V. Dmitriev, and V.B. Eltsov, presented in QFS2018.
- [26] D.A.Ivanov, Phys. Rev. Lett. **86**, 268 (2001); G. E. Volovik, JETP Lett.**70**, 609 (1999).